

Suppressing one-bond homonuclear ^{13}C , ^{13}C scalar couplings in the J-HMBC NMR experiment: Application to ^{13}C site-specifically labeled oligosaccharides

Robert Pendrill, Ole W. Sørensen[♦] and Göran Widmalm*

Department of Organic Chemistry, Arrhenius Laboratory, Stockholm University, S-106 91 Stockholm, Sweden

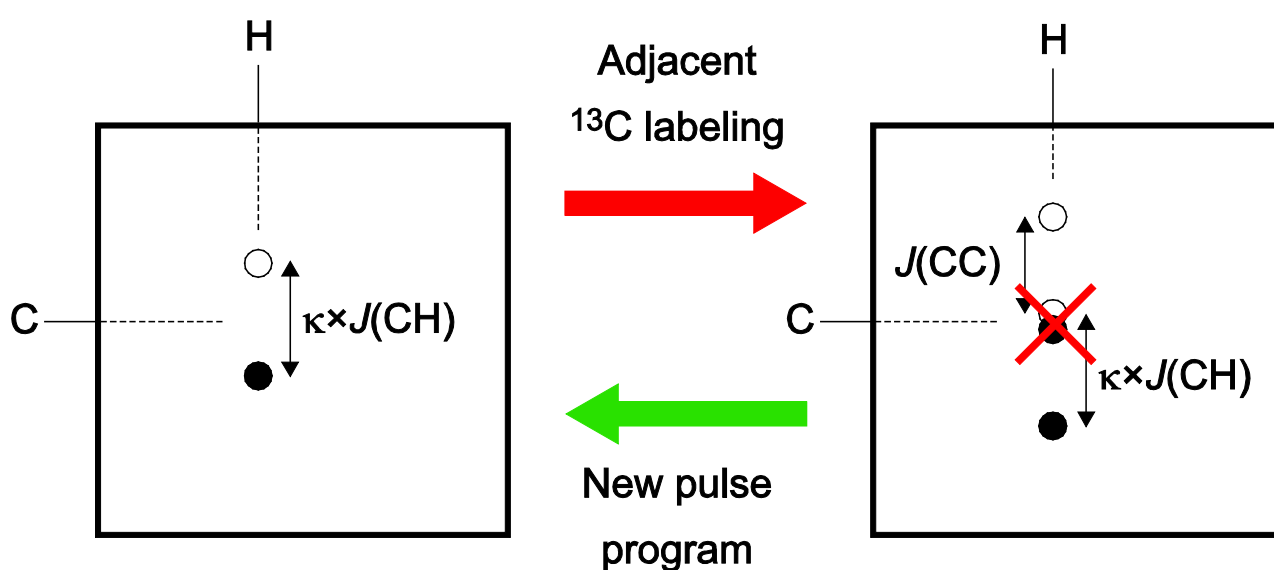
[♦]sorensen.ole.w@gmail.com

*Corresponding author. E-mail: gw@organ.su.se

Keywords: NMR; ^1H ; ^{13}C ; J-HMBC; oligosaccharide; heteronuclear long-range coupling constants; site-specific labeling

TOC text

The determination of heteronuclear long-range coupling constants using the J-HMBC experiment is problematic when site-specific ^{13}C labeling has been introduced adjacent to the carbon involved in the coupling pathway, as demonstrated for three oligosaccharides. Two different modifications of the J-HMBC pulse sequence are suggested and both are shown to result in spectra free from disturbance by suppressing the evolution of homonuclear ^{13}C , ^{13}C scalar couplings.



Abstract

Site-specific ^{13}C isotope labeling is a useful approach that allows for the measurement of homonuclear ^{13}C , ^{13}C coupling constants. For three site-specifically labeled oligosaccharides it is demonstrated that using the J-HMBC experiment for measuring heteronuclear long-range coupling constants is problematical for the carbons adjacent to the spin label. By incorporating either a selective inversion pulse or a constant-time element in the pulse sequence, the interference from one-bond ^{13}C , ^{13}C scalar couplings is suppressed, allowing the coupling constants of interest to be measured without complications. Experimental spectra are compared to spectra of a non-labeled compound as well as simulated spectra. The work extends the use of the J-HMBC experiments to site-specifically labeled molecules, thereby increasing the number of coupling constants that can be obtained from a single preparation of a molecule.

Introduction

The investigation of molecular conformation by NMR spectroscopy depends to a large extent on the measurement of scalar coupling constants. In particular, long-range coupling constants often carry information on torsion angle preferences.^[1-3] For the measurement of heteronuclear long-range coupling constants, a powerful method is the J-HMBC experiment which allows the measurement of many such coupling constants in one single experiment.^[4] In the J-HMBC experiment, heteronuclear ^{13}C , ^1H long-range coupling constants appear in the indirect dimension as anti-phase doublets centered at the frequencies of the involved carbon nuclei. The associated peak splitting is scaled by an adjustable factor, allowing accurate measurements of coupling constants without the need for an impractical number of increments in the indirect dimension.

In cases where the measurement of homonuclear ^{13}C , ^{13}C coupling constants is desired, site-specific isotope labeling is a useful approach to offset the low sensitivity caused by the low natural abundance of ^{13}C nuclei.^[5,6] The carbon atoms adjacent to the labeled position(s) will be affected by one-bond carbon-carbon ($^1J_{\text{CC}}$) coupling constants, which in the J-HMBC experiment will give rise to an additional in-phase splitting in the indirect dimension. If this additional splitting is of comparable magnitude to the scaled heteronuclear coupling constant, cancellation of peaks will occur, making the measurement difficult and leaving room for misinterpretation.

Two common approaches for the suppression of coupling constant evolution in 2D NMR experiments are the use of frequency-selective pulses^[7] and constant-time pulse sequences.^[8] Using these strategies, we have developed two modifications of the J-HMBC experiment to remove the

influence of interfering homonuclear ^{13}C , ^{13}C scalar couplings, thereby extending the scope of the J-HMBC experiment to site-specifically labeled molecules. Their use is demonstrated for a selection of site-specifically labeled oligosaccharides (Figure 1).

Results and Discussion

Our new experiments extend the J-HMBC pulse sequences of Meissner and Sørensen^[4] by the two options for suppression of the evolution under homonuclear carbon-carbon couplings during the evolution period as outlined in Figure 2.

The simplest modification, shown in Figure 2a, is the introduction of a frequency-selective π pulse applied at the frequency of the labeled carbon simultaneously with the proton π pulse in the middle of the evolution period, thus refocusing couplings to all other carbons not affected by the pulse.

As an alternative, the sequence shown in Figure 2b was devised, in which the evolution of the aforementioned homonuclear carbon-carbon coupling constants is suppressed by keeping the length of the evolution period constant. This constant-time element has also been used in HMQC-type experiments^[9,10] and ensures refocusing of evolution under proton chemical shifts as well as heteronuclear coupling constants for the pertinent multiple-quantum coherences in the evolution period. The homonuclear carbon-carbon coupling constant makes the signal intensity proportional to $\cos(\pi \times J_{\text{CC}} \times T)$ and thus the length of the constant-time period should be set close to a multiple of $1/J_{\text{CC}}$ for maximum sensitivity.

The use of the pulse sequences for the measurement of coupling constants related to the conformationally important torsion angle ψ is demonstrated in Figures 3-5. For the $[2'\text{-}^{13}\text{C}]$ site-specifically labeled disaccharide **G2G**, the region pertaining to the ${}^3J_{\text{C1',H2}}$ of the J-HMBC spectra obtained with the original pulse sequence using two different scaling factors are shown in Figure 3a,c. The additional in-phase splitting is clearly visible when the larger scaling factor is used, while the inner components cancel at the smaller scaling factor. In the latter case, it is not possible to determine the value of the coupling constant directly from the spectrum. However, when using the constant-time sequence shown in Figure 2b, the interference from ${}^1J_{\text{CC}}$ is suppressed, revealing the actual value of the coupling constant (Figure 3b,d), 4.2 Hz for both scaling factors, as previously reported.^[11]

For the $[2'\text{-}^{13}\text{C}]$ site-specifically labeled disaccharide **G3G**, Figure 4 shows 1D projections of the 2D spectra resulting from the different pulse sequences and scaling factors. The measurement of the ${}^3J_{\text{H1',C3}}$ coupling constant is hampered by the ${}^1J_{\text{CC}}$ when the original pulse sequence is used (Figure 4a and b). Using the smaller scaling factor, the appearance is deceptively similar to a spectrum

obtained without interference and there is a clear risk of the peak separation erroneously being judged as arising only from the heteronuclear coupling constant, the value of which in this case would be severely overestimated. The true value of the coupling constant is revealed (Figure 4c and d) using the pulse sequence shown in Figure 2b, of 4.7 Hz and 4.8 Hz for the small and large scaling factor, respectively, compared to the literature value of 4.8 Hz.^[11] Overlaid in red in Figure 4 are spectra obtained from simulation using the original pulse sequence and the same parameters as in experiment. Indeed, the interference is well reproduced by simulation (Figure 4a and b), and the spectra obtained by leaving out the [2'-¹³C] nucleus from the simulation (Figure 4c and d) are essentially identical to the ones obtained experimentally using the pulse sequence in Figure 2b together with the labeled compound.

The pulse sequence in Figure 2a was used together with a frequency-selective pulse to attain suppression of the ¹J_{CC} couplings in the trisaccharide **R23** (Figure 1). It is clearly seen from Figure 5 that the resulting spectrum (b) is equivalent to that obtained by using either the pulse sequence in Figure 2b (shown in c) or by using the non-labeled compound together with the original pulse sequence (d), whereas the spectrum (a) obtained with the original pulse sequence and the labeled compound again demonstrates the interference from the homonuclear carbon-carbon coupling constant. From all spectra except for (a), it is possible to extract a value for the coupling constant in agreement with the previously reported value of 5.2 Hz.^[12]

As always in constant-time spectroscopy the sensitivity gain due to simplified multiplet structure can in molecules with short *T*₂ values be offset by relaxation loss during the constant-time delay. However, given that the excitation delay Δ already has to be quite long to resolve small heteronuclear long-range coupling constants the additional constant-time delay to suppress ¹³C, ¹³C coupling constants only represents a relatively small extension of the pulse sequence compared to the original version.

In conclusion, the J-HMBC sequence has been modified to afford suppression of homonuclear ¹³C, ¹³C couplings which interfere with the measurement of conformationally important long-range heteronuclear coupling constants. Two alternative sequences have been developed, and their effectiveness has been demonstrated on site-specifically labeled oligosaccharides and it is envisioned that these sequences will be useful when the non-labeled analogue of a compound is not at hand but the couplings involving carbons adjacent to the labeled position are still of interest.

Experimental

General. Simulations of NMR experiments were performed using the NMR-SIM program (Bruker,

v. 5.4 for Linux) using the same pulse sequences and parameters as used experimentally. Minimal spin systems containing C1' and C2' together with the proton involved in the coupling as well as its vicinal proton coupling partners were used, with chemical shifts and coupling constants as determined from experiment. Primes denote atoms in non-reducing residues. The site-specifically labeled disaccharides β -D-[2'- ^{13}C]Glc p -(1 \rightarrow 2)- α -D-Glc p -OMe (**G2G**) and β -D-[2'- ^{13}C]Glc p -(1 \rightarrow 3)- α -D-Glc p -OMe (**G3G**)^[11] as well as the trisaccharide α -L-[2'- ^{13}C]Rhap-(1 \rightarrow 2)[α -L-[2''- ^{13}C]Rhap-(1 \rightarrow 3)]- α -L-Rhap-OMe (**R23**)^[12] were available from previous studies.

NMR spectroscopy. Freeze-dried samples of **G2G** and **G3G** were dissolved D₂O (0.6 mL), giving concentrations of 52 and 51 mM, respectively. The preparation of NMR samples containing **R23** has been described previously.^[12] Experiments were performed at 298 K for the disaccharides and at 310 K for the trisaccharide on a 700 MHz Bruker Avance III spectrometer. The spectrometer was equipped with a 5 mm TCI Z-gradient CryoProbe. The J-HMBC experiments were recorded with a third order low-pass *J*-filter ($\tau_1 = 3.45$ ms, $\tau_2 = 3.13$ ms and $\tau_3 = 2.78$ ms).^[4] The direct dimension was sampled for 0.58 s with a spectral window of 5 ppm while the indirect dimension was sampled over 60 ppm using 288 or 512 t_1 increments with 8 – 32 transients per increment in echo/anti-echo mode. For the larger scaling factors ($\kappa = 33.3$ and 18.8), the coupling evolution delay (Δ) was set to 455 ms and for the smaller factor ($\kappa = 11.5$) the delay Δ was 278 ms. Scaling factors were calculated from $\kappa = \Delta/t_1^{\text{max}}$. Carbon-13 inversion during the coupling evolution was performed using a 60 kHz smoothed Chirp pulse (0.5 ms, 20.1% smoothing) while refocusing during chemical shift evolution was performed by a 60 kHz composite smoothed Chirp pulse (2 ms). For the J-HMBC experiments with selective inversion at the labeled carbon, a 10 ms Gaussian pulse was applied at the center of the t_1 period. In the experiments utilizing the pulse sequence in Figure 2b, the constant-time delay was set to 44.4 ms (i.e. $T = 2/{}^1J_{\text{CC}}$ assuming a value of 45 Hz for ${}^1J_{\text{CC}}$). Pulsed field gradients were set to 18%, -10%, -5%, -3% of the maximum, being 50 G \cdot cm⁻¹, for the low-pass filter and 80%:-48% and -48%:80% for echo/anti-echo selection. The data matrices were zero-filled to at least 16k data points in the indirect dimension and multiplied by squared cosine-bell window function prior to Fourier transformation and subsequent transformation into the power spectrum, allowing 1D projections to be obtained. From these, the coupling constant values were calculated by $J = \Delta_{F_1}/\kappa$, with Δ_{F_1} being the measured peak separation.

Acknowledgements

This work was supported by grants from the Swedish Research Council and the Knut and Alice Wallenberg Foundation.

References

1. T. Rundlöf, A. Kjellberg, C. Damberg, T. Nishida, G. Widmalm, *Magn. Reson. Chem.* **1998**, *36*, 839.
2. N. Nath, Lokesh, N. Suryaprakash, *ChemPhysChem* **2012**, *13*, 645.
3. J. Saurí, T. Parella, *Magn. Reson. Chem.* **2013**, *51*, 397.
4. A. Meissner, O. W. Sørensen, *Magn. Reson. Chem.* **2001**, *39*, 49.
5. C. A. Podlasek, J. Wu, W. A. Stripe, P. B. Bondo, A. S. Serianni, *J. Am. Chem. Soc.* **1995**, *117*, 8635.
6. K. H. M. Jonsson, E. Säwén, G. Widmalm, *Org. Biomol. Chem.* **2012**, *10*, 2453.
7. R. Brüschweiler, C. Griesinger, O. Sørensen, R. Ernst, *J. Magn. Reson.* **1988**, *78*, 178.
8. A. Bax, R. Freeman, *J. Magn. Reson.* **1981**, *44*, 542.
9. T. Szyperski, C. Fernández, A. Ono, K. Wüthrich, M. Kainosho, *J. Magn. Reson.* **1999**, *140*, 491.
10. K. Hu, W. M. Westler, J. L. Markley, *J. Biomol. NMR* **2011**, *49*, 291.
11. U. Olsson, A. S. Serianni, R. Stenutz, *J. Phys. Chem. B* **2008**, *112*, 4447.
12. K. H. M. Jonsson, R. Pendrill, G. Widmalm, *Magn. Reson. Chem.* **2011**, *49*, 117.

Figure legends

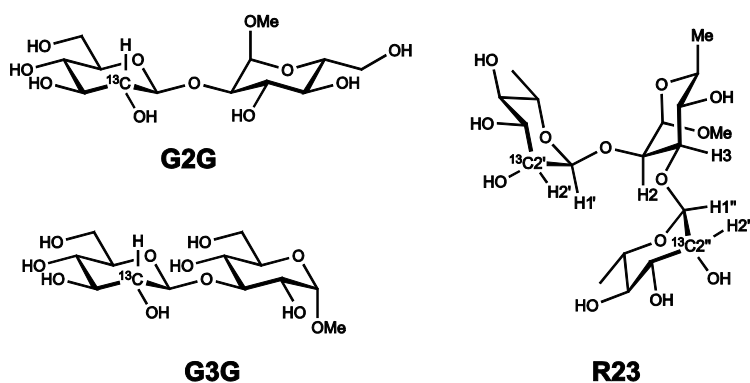


Figure 1. Schematic of the site-specifically ^{13}C labeled oligosaccharides used in this study.

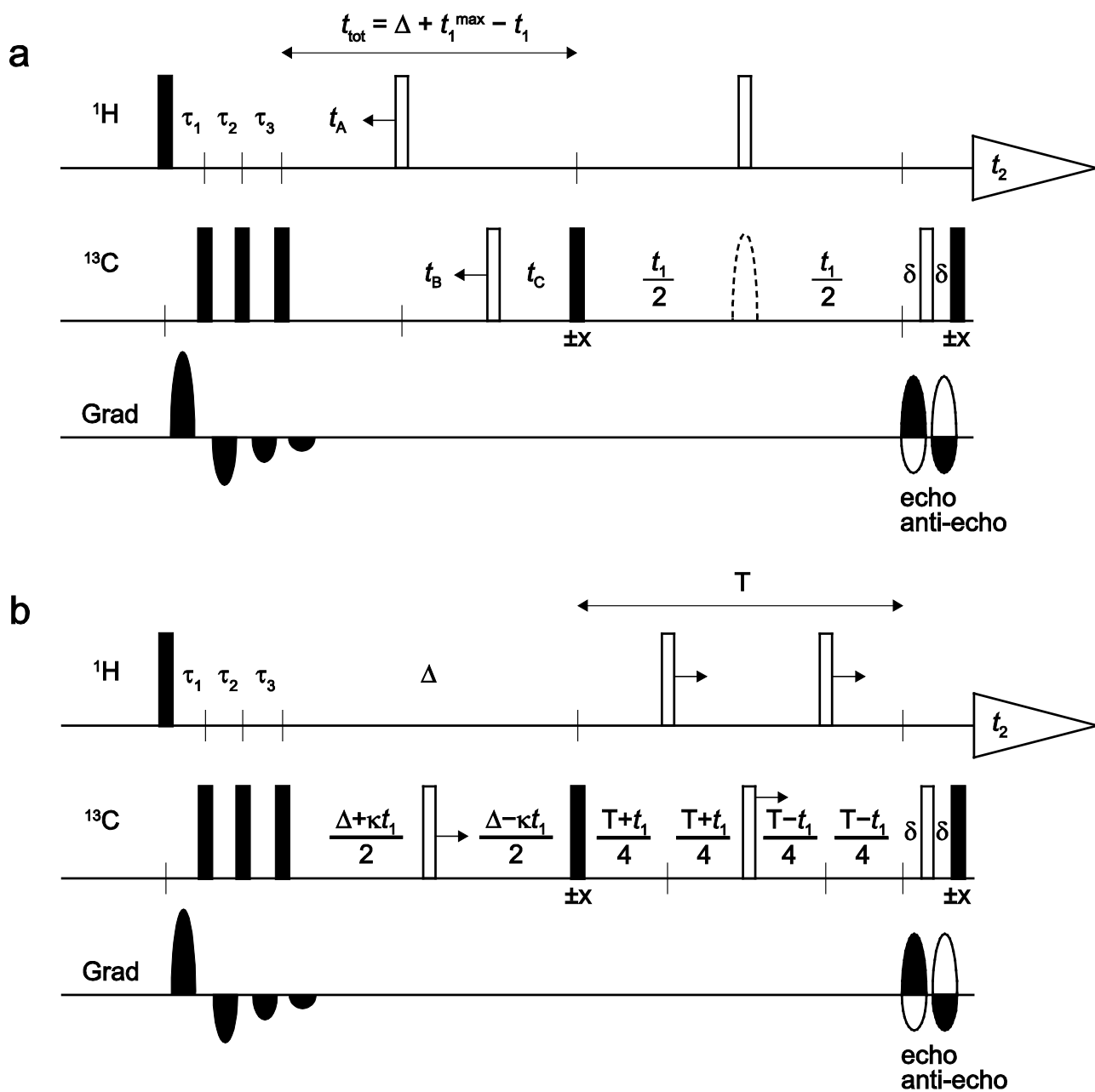


Figure 2. Graphical overview of the pulse sequences. (a) The constant-time J-HMBC for the suppression of $J_{\text{H,H}}$ coupling constants,^[4] with the placement of a frequency-selective pulse for suppression of homonuclear carbon-carbon coupling constants shown as a dashed half-ellipse. (b) Constant-time experiment for the suppression of J_{CC} coupling constants.

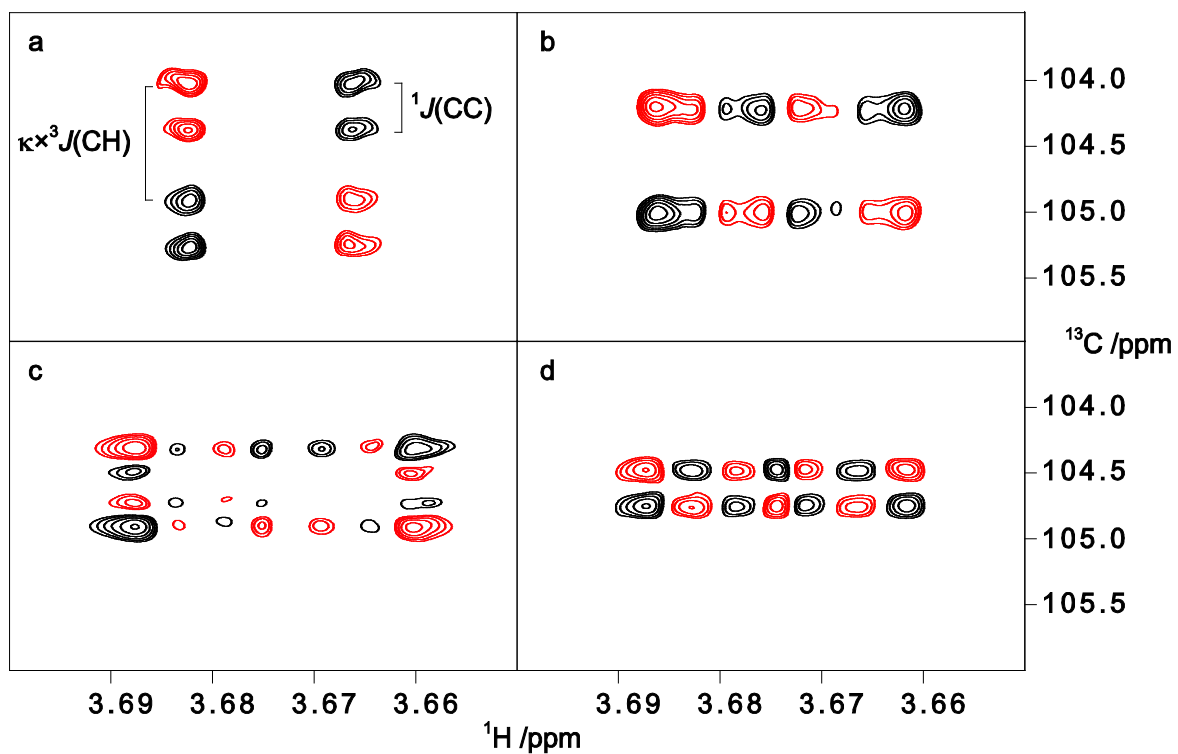


Figure 3. Two-dimensional spectra obtained for **G2G** using two different scaling factors and the sequences shown in Figure 2. The region related to ${}^3J_{C1',H2}$ is shown with the scaling factor set to 33.3 together with (a) the pulse sequence in Figure 2a (without the frequency-selective pulse) and (b) the pulse sequence in Figure 2b. Corresponding spectra obtained using the scaling factor 11.5 are shown in (c) and (d), respectively.

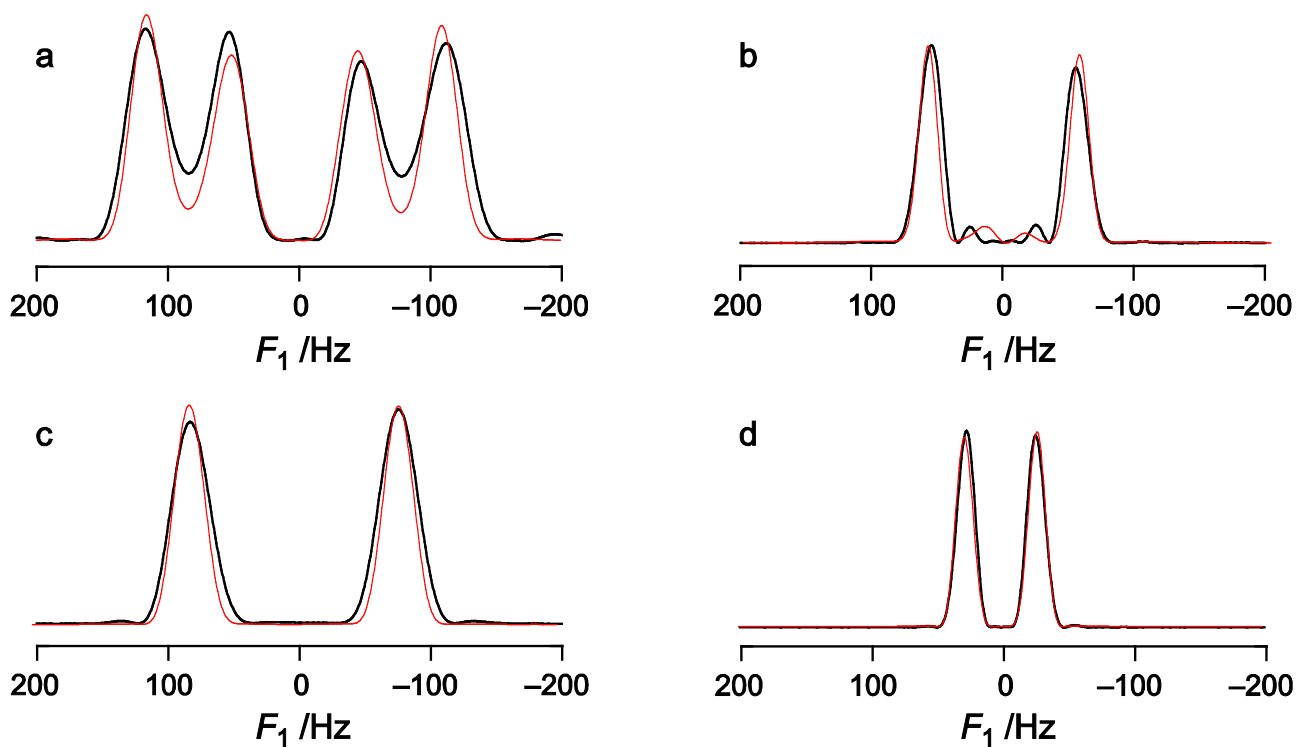


Figure 4. One-dimensional projections of experimental spectra obtained using two different scaling factors for **G3G** using pulse sequences in Figure 2, corresponding to the scaled ${}^3J_{C1',H3}$ coupling constant. (a) and (b) using the sequence in Figure 2a (without the frequency-selective pulse) and scaling factors 33.3 and 11.5 respectively. (c) and (d), the corresponding spectra obtained using the sequence in Figure 2b. Shown in red color are the simulated spectra using the pulse sequence in Figure 2a (without the frequency-selective pulse) together with labeled **G3G** in (a) and (b) and unlabeled **G3G** in (c) and (d).

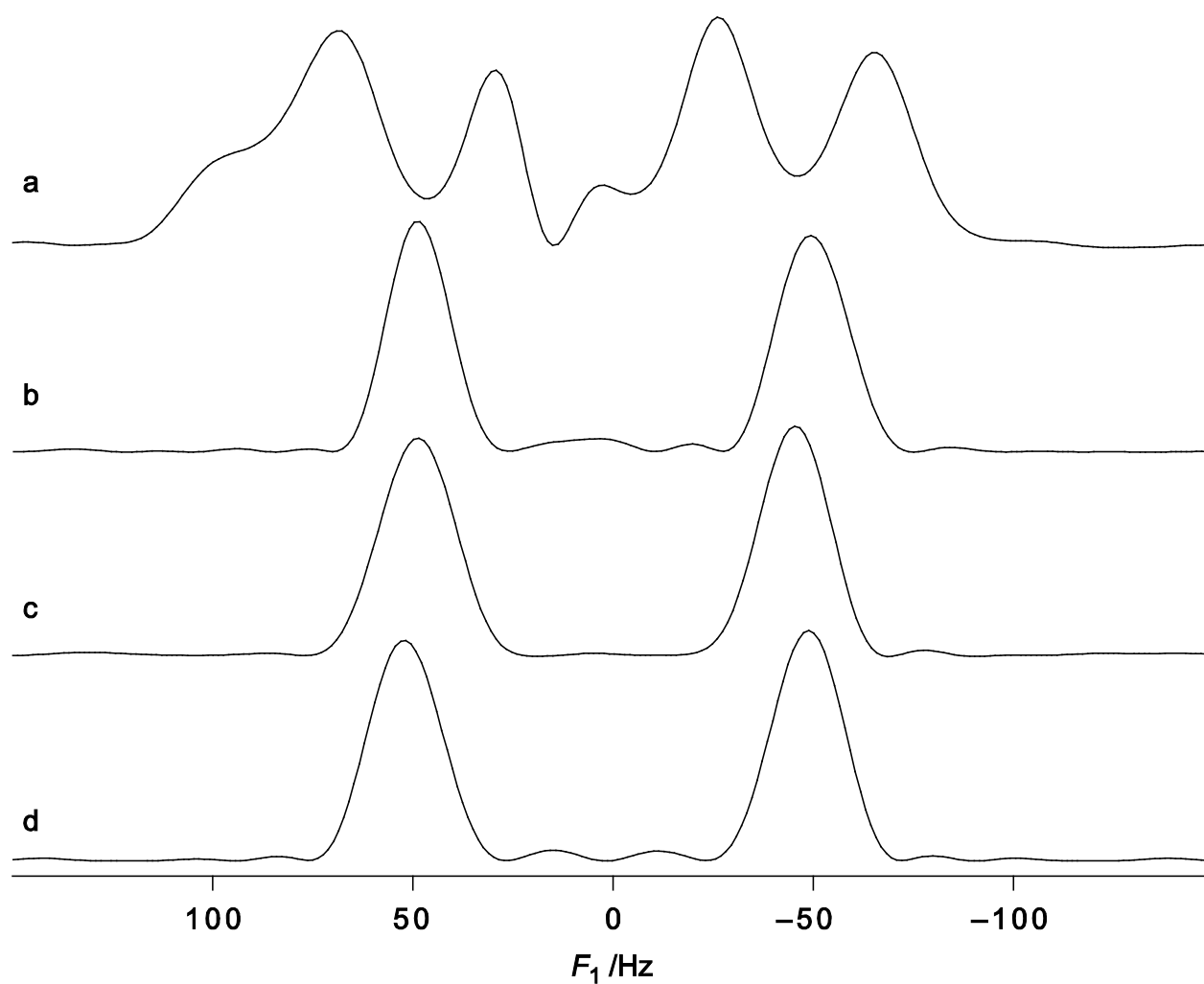


Figure 5. One-dimensional projections of spectra obtained for **R23** using a scaling factor of 18.8 and three different pulse sequences, showing the section relevant for ${}^3J_{C1'',H3}$; (a) Figure 2a without the frequency-selective pulse, (b) Figure 2a together with a frequency-selective pulse and (c) Figure 2b. (d) The spectrum obtained using the sequence in Figure 2a (without the frequency-selective pulse) for the unlabeled compound.